The effect of the acquisition parameters for High Angular Resolution Diffusion Imaging

V. Prckovska[1], A. F. Roebroeck[2], P. W. Pullens[2,3], A. Vilanova[4], and B. M. ter Haar Romeny[4]

[1]Biomedical Engineering, Technical University of Eindhoven, Eindhoven, Netherlands, Netherlands, [2]Maastricht Brain Imaging Center, Dept. of Cognitive Neuroscience, Faculty of Psychology, Maastricht University, Maastricht, Netherlands, [3]Brain Innovation B.V., Maastricht, Netherlands, [4]Biomedical Engineering, Technical University of Eindhoven, Eindhoven, Netherlands

INTRODUCTION: One of the recent challenges in diffusion imaging is to find acquisition schemes and analysis approaches that can represent non-Gaussian diffusion profiles in a clinically feasible measurement time. In this work we investigate the effect of the b value and the number of gradient vector directions on the HARDI models Q-ball imaging and the Diffusion Orientation Transform (DOT) in a structured way using computational simulations, hardware crossing-fiber diffusion phantoms, and in-vivo brain scans. We quantify the angular resolution of the reconstructed probability profiles under different acquisition schemes. We vary the b value and number of gradients directions to investigate their effects and interaction. Knowledge of the suitable acquisition parameters in clinical setting, for different HARDI diffusion models, where still satisfying results are obtained given the high noise impact on the data, is of significant importance in this emerging area.

METHODS: We implemented the analytical Q-ball imaging [1] and the parametric and nonparametric DOT [2] in C++. As the results of DOT depend on the optimal radius of the sphere that defines the probability function R_0 and the effective diffusion time t, we experimentally found R_0 and extracted t from the imaging parameters as $t = \Delta - \delta/3$. In our simulations we found the following values of $R_0 = \{22, 24, 26, 28, 30\}\mu m$ to give minimal angular error for the DOT. We varied the order of the Spherical Harmonics *l*, between 4 and 8. As a preprocessing step for the noisy data sets, we included Laplace-Beltrami (LB) smoothing on the signal, for both of the methods with $\lambda = 0.006$ as in [3]. We assume that the fiber directions are given by the local maxima of the normalized [0,1] ODF/probability profile where the function surpasses a threshold (0.5 like in [1]).

DATA: Synthetic data of 2-fiber crossings under 40°, 45°, 50°, 55°, 60° and 90° were generated in Mathematica by simulating the DW-MR signal attenuation from molecules restricted inside a cylinder [4]. Gaussian noise was added to the real and complex part of the signal with realistic SNR corresponding to the used b values (15.3, 14.1, 13.3, 12.0 and 11.9 for 1000, 1500, 2000, 3000 and 4000 s/mm^2 respectively). DW-MRI hardware phantoms were constructed of 2-fiber crossings under 30°, 50°, and 65° [5]. DW-MRI acquisition was performed on subject VP (25 yrs, female) using a twice refocused SE-EPI sequence on a Siemens Allegra 3T (Siemens, Erlangen). FOV 208× 208 mm, voxel size 2.0× 2.0× 2.0mm. 10 horizontal slices were positioned through the body of the *corpus callosum* and *centrum semiovale*. Data sets were acquired with #vols(#dirs): 132(120) 106(96), 80(72), 54(48) directions, each at b values of 1000, 1500, 2000, 3000, 4000 s/mm2. The phantom was scanned using exactly the same DW-MRI protocol as the human subject (the 54 directions scheme was omitted from the protocol).

a) Gradient directions

Simulated angle	40°	45°	50°	55°	60°	90°
54	l=6;b=1000	l=6;b=1000	l=4;b=2000 l=6;b=1000	l=4;b=1000	l=4;b=1000	l=4;b=1000
80	l=6;b=1000	l=6;b=1000	l=4;b=2000 l=6;b=1000	l=4;b=1000	l=4;b=1000	l=4;b=1000
106	l=6;b=1000	l=6;b=1000	l=4;b=2000 l=6;b=1000	l=4;b=1000	l=4;b=1000	l=4;b=1000
132	l=6;b=1000	l=6;b=1000	l=4;b=2000 l=6;b=1000	l=4;b=1000	l=4;b=1000	l=4;b=1000
Estimated angle	36,7313°	47,5762°	52,5901°	52,5901°	60,5194°	89,3214°

b) Gradient directions

Simulated angle	40°	45°	50°	55°	60°	90°
54	l=8;b=2000	l=6;b=3000 l=8;b=1500	l=6;b=2000 l=8;b=1500	l=6;b=1000	l=4;b=2000 l=6;b=1000	l=4;b=1000
80	l=8;b=1500	l=6;b=3000 l=8;b=1500	l=6;b=2000	l=6;b=1000	l=4;b=2000 l=6;b=1000	l=4;b=1000
106	l=8;b=1500	l=6;b=4000 l=8;b=1500	l=6;b=2000	l=6;b=1000	l=4;b=2000 l=6;b=1000	l=4;b=1000
132	l=8;b=1500	l=6;b=3000 l=8;b=1500	l=6;b=2000	l=6;b=1000	l=4;b=2000 l=6;b=1000	l=4;b=1000
Estimated angle	36.7313	47.5762	52.5901	52.5901	60.5194	89.3214

Figure 1. Results from the noiseless simulations.

RESULTS: In noiseless simulation (Fig. 1), DOT gives the same results as Q-ball but at lower b value and less gradient directions. On Fig. 2 and Fig. 3, results of the noisy synthetic and hardware phantom data analysis are given. The angular error is plotted for the smallest angle found within our criteria (the angular error and the standard deviation to be smaller than a liberate threshold of 20), for each combination of b value and direction table (given on the x-axis), both for DOT (upper panel) and Q-ball (lower panel). On Fig.2 we observe that DOT recovers in most of the cases smaller angles than Q-ball for the same set of acquisition parameters. Fig. 3 shows that DOT manages to recover most of the simulated angles over different set of acquisition parameters, and generally with lower angular error than Q-ball. Even

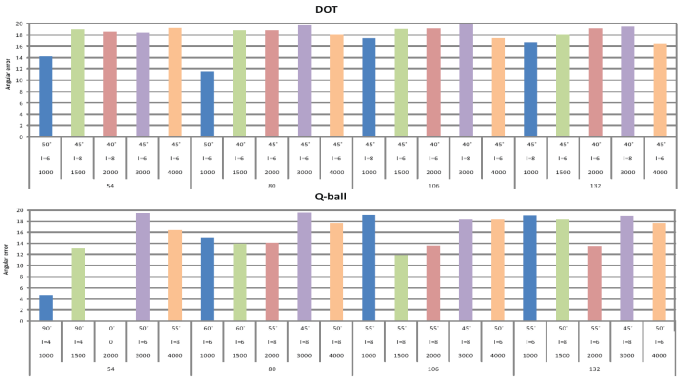

Figure 2. Results from the noisy synthetic data. On x-axis from top to bottom: best detected angle, order *l*, b value and number of grad. directions.

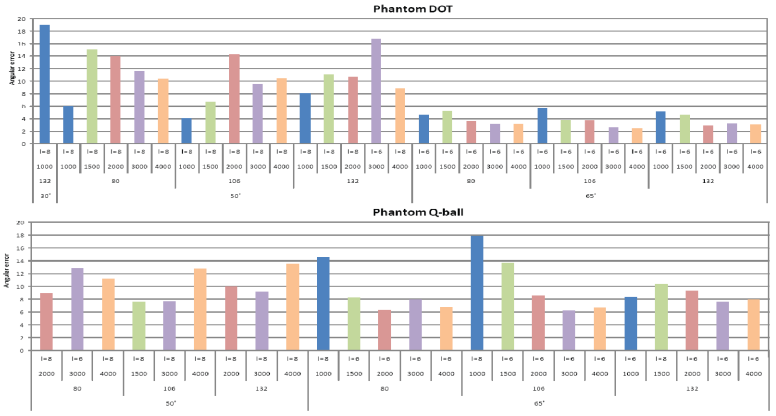

Figure 3. Results from the hardware phantom data. On x-axis from top to bottom: order *l*, b value, number of gradient directions and simulated angle.

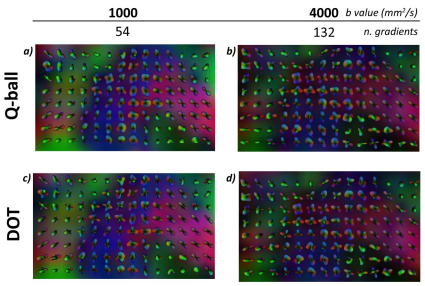

Figure 4. *In vivo* results of the brain area of *corpus callosum* and *corona radiate*.

b-value (s/mm^2)	1000		1500		2000	
R_0 (mm) \ *l*	6	8	6	8	6	8
22			12.2326	11.8887	10.3561	9.06114
24	14.8464	11.7853	9.39503	8.0394	10.5807	7.27885
26	9.53001	7.63227	10.206	6.16571	10.3153	5.90953
28	6.73422	5.15169	9.77987	5.36415	11.2252	5.24265
30	7.09634	4.71809		4.50026	10.9818	5.11423

Figure 5. Dependence of the angular error on b value, R_0 and *l* order.

an angle of 30° of crossings is detected by the DOT at a cost of high *l* and number of gradients. The results from *in-vivo* data show more details in DOT glyphs independently of the b value and number of gradients (Fig. 4). The table on Fig. 5 summarizes the results of the angular error from unsmoothed DOT with standard deviation less than 20, for different combinations of b value (1000-2000 s/mm^2), *l* order and radius R_0 over 100 noise realizations for simulated 60° of crossing and 132 gradient directions. We run experiments of varying the LB smoothing parameter λ over the interval of [0.001;1]. LB smoothing on the signal improves the results only in the cases marked with green on the table in Fig. 5, by 1 or 2°, for λ around 0.002.

CONCLUSION: Our results suggest that over a wide range of acquisition schemes DOT can outperform Q-ball in realistic simulations, hardware diffusion phantom data and *in-vivo* brain data. However tuning the optimal R0 for the DOT, is not trivial in in-vivo data sets, and by simplicity and speed of calculations of the reconstructed ODFs, Q-ball still has a significant advantage. In this work we also explored the effect of LB smoothing on the signal for DOT. The signal attenuation in DOT is assumed to be mono-exponential for b <2000 s/mm^2, which can be seen as a smoothing in q-space already. Therefore LB smoothing slightly improves the properties of DOT in some specific cases (Fig. 5). Knowledge of suitable acquisition schemes in a clinical setting, that can correctly estimate non-Gaussian diffusion profiles for HARDI, can improve the utility of DW-MRI for the diagnosis of white matter diseases and presurgical planning.

References: [1] Descoteaux et al, MRM 2007; [2] Ozarslan et al, NeuroImage 2006; [3] Descoteaux et al, MRM 2006; [4] Soderman et al, MRM 1995; [5] Pullens et al, ISMRM 2007